2-2-2013

A Computational Approach to Optimize Microring Resonators for Biosensing Applications

Justin C. Wirth
Birck Nanotechnology Center, Purdue University, jcwirth@purdue.edu

B. R. Wenner
Birck Nanotechnology Center, Purdue University

M. S. Allen
Birck Nanotechnology Center, Purdue University

J. W. Allen
Birck Nanotechnology Center, Purdue University

M. Qi
Birck Nanotechnology Center, Purdue University

Wirth, Justin C.; Wenner, B. R.; Allen, M. S.; Allen, J. W.; and Qi, M., "A Computational Approach to Optimize Microring Resonators for Biosensing Applications" (2013). *Birck and NCN Publications.* Paper 1325.
http://dx.doi.org/10.1117/12.2001820

A Computational Approach to Optimize Microring Resonators for Biosensing Applications

J.C. Wirth[1], B.R. Wenner[2,3], M.S. Allen[2], J.W. Allen[2], M. Qi[1]
[1]Purdue University, Birck Nanotechnology Center, 1205 West State Street, West Lafayette, Indiana 47907
[2]Sensors Directorate, Air Force Research Laboratory, Wright-Patterson AFB, OH 45433

[3]Contact: brett.wenner@wpafb.af.mil

ABSTRACT

Microcavity structures have recently found utility in chemical/biological sensing applications. The appeal of these structures over other refractive index-based sensing schemes, such as those based on surface plasmon resonance, lies in their potential for producing a highly sensitive response to binding events. High-Q devices, characterized by sharp line widths, are extremely attractive for sensing applications because the bound analyte provides an increased optical pathlength, thus shifting the resonant frequency of the device. In this work, we design and simulate resonant microrings using full-wave finite element models. In addition to structure design, integration of the biological recognition element on the resonator is also considered. This is equally important in dictating the sensitivity of the sensing device. To this end, we take a four-step theoretical approach to optimizing the sensor. We begin by using FEM analysis to obtain the characteristic resonant wavelength, line width, and quality factor for bare ring resonators absent of surface functionalization. Next, we simulate the structure with a biorecognition element attached to the surface. The third step is to model the functionalized microring to mimic the interaction with the target analyte. At each step, we derive the transmission spectra, electric field distributions and coupling efficiencies, as well as wavelength dependence using empirical data for the refractive indices of biorecognition element and analyte. Finally, the geometry of the microrings is optimized in conjunction with the constituent material properties and the recognition chemistry using FEM combined with an optimization algorithm to maximize the sensitivity of the integrated biosensor.

Keywords: biosensing, ring resonator, microcavity, silicon photonics

1. INTRODUCTION

Microcavity resonators offer the ability to confine light in a small area, and the very low loss achievable by dielectric waveguides such as silicon (Si) or silicon nitride (SiN) on silicon dioxide (SiO_2) substrates lead to very high Q values and narrow line widths[1,2]. In particular, microring resonators allow for a small footprint, easy fabrication, and relatively simple designs[2]. These structures have seen use in a variety of applications, including many optical devices that previously required large bulk optical setups[2]. Normally, these resonators are designed to have a tight confinement of light to minimize propagation loss and work at a polarization that matches the waveguide geometry[1]. However, with mild tweaking, these structures can retain their low loss characteristics, but also increase the delocalization of the confined mode. This modal delocalization, combined with the narrow line width and high environmental sensitivity of the microcavity, can be used for refractive index difference based detection[3]. Baseline resonant behavior of a resonator is measured and then compared to the behavior of the cavity when an object with different refractive index is introduced near the cavity. For ring resonators, this object will result in a shift in the effective modal index, and will consequently change the resonant wavelength of the cavity. This resonant shift can thus be used as a sensing mechanism.

Although ring resonators have been explored for chemical/biological detection[4], little work has been done to optimize the sensing effect in a systematic way. Typically, the microrings are operated as they would be for a photonic device, which usually means a standard waveguide dimension and operation in the quasi-TE polarization[5], which confines the mode very well. While these sorts of microring designs make very much sense for typical optical devices, they do not make sense for optical sensing. As opposed to traditional photonic devices, photonic sensors rely on modal

Frontiers in Biological Detection: From Nanosensors to Systems V, edited by Benjamin L. Miller, Philippe M. Fauchet, Proc. of SPIE Vol. 8570, 857001
 · doi: 10.1117/12.2001820

delocalization for their function[2,6], while this is normally avoided for photonic devices. Therefore, there is much room to optimize the microring structures for the particular application of biological sensing.

In this work, we attempt to optimize a ring resonator structure for use in biological sensing. Although this could be used for sensing of liquids, molecules, proteins, or any other structure which can be shown to have a differing refractive index from a baseline, we consider here detection of a cell. The main ring parameters of material, waveguide dimensions, modal polarization, wavelength, and coupling gap are all explored. As the microring is a three dimensional structure, a full three dimensional model is necessary to obtain a prediction of the device performance. However, we first consider the cross section of the ring, and optimize the waveguide, material, polarization, and wavelength to allow for maximal sensitivity. Using these optimized parameters, we then simulate the transmission spectra of the partially optimized ring, and then further optimize the ring coupling parameters for maximum sensing performance.

2. RING RESONATOR DESIGN CONSIDERATIONS

A microring resonator based sensor capitalizes on the very sensitive resonant behavior of the ring and sensitivity to small changes of and around the cavity. Detection of an object of interest is accomplished by noting a shift in the resonant wavelength of the ring, given by[4]:

$$\Delta\lambda_m = \Delta n_{eff}\left(\frac{L}{m}\right)$$

where $\Delta\lambda_m$ is the resonant wavelength shift of the ring mode, $\Delta n_{eff,m}$ is the effective index difference of guided mode m between the reference and sensing situations, L is the total length of the ring, and m is the number of mode wavelengths present in the ring during resonance. The ratio $\left(\frac{L}{m}\right)$ will vary with the wavelength of light used, but will otherwise be constant. Therefore, the sensing response of the microring mainly depends on the difference of effective index due to the object to be sensed, which is given by[7]:

$$\Delta n_{eff,m} = c\iiint \Delta\varepsilon(x,y,z)\vec{E}_m(x,y,z)\cdot\vec{E}_m^*(x,y,z)dxdydz$$

where c is the speed of light, $\Delta\varepsilon(x,y,z)$ is the change in relative permittivity at a point *(x,y,z)* due to the analyte, and $\vec{E}_m$ is the electric field of mode m at point (x,y,z). The integrand can be seen to be the energy density $(\vec{D}\cdot\vec{E})$ present in the vicinity of the waveguide.

To maximize the resonant wavelength shift, the change in effective index due to a given analyte should be maximized. This can be achieved by maximizing the amount of modal field that experiences the relative permittivity difference due to the sensing element. This requires an optimization of the modal profile to the shape, size, location, and material of the object to be sensed. Since the field outside the waveguide roughly falls off in direction l as[7]:

$$e^{-l\frac{2\pi}{\lambda}\sqrt{n_{eff}^2-n_{outer}^2(x,y,z)}}$$

where n_{eff} is the effective modal refractive index, and $n_{outer}$is the refractive index of the material outside the waveguide core, the index contrast between the mode (which is dominated by the waveguide index) and the surrounding material will dictate how quickly the mode decreases away from the waveguide. A large contrast will result in very quick falloff, and low contrast will result in decreased falloff. Since normal electric displacement field is constant across a dielectric boundary, and $\vec{D}=\varepsilon\vec{E}$, there will be an enhanced electric field across the dielectric boundary parallel to the modal polarization dependent on the boundary index difference.

In addition to the waveguide material and modal polarization, the waveguide dimensions and modal wavelength play a large role in the behavior of the modal profile. Decreasing either the height or width of the waveguide will generally lead to a less confined mode. Similarly, increasing the modal wavelength will cause the mode to be less confined in a waveguide of fixed dimensions.

Sensing performance is not only dependent on resonant shift, but is also affected by the achievable quality (Q) factor of the resonant cavity. A larger Q will lead to more narrow resonant peaks, increasing the ease of which a wavelength shift can be detected. There is generally a tradeoff between modal confinement and losses, which is why highly confined modes are generally desired[2]. For biological sensing in the infrared, there is the additional issue related to the absorption

spectrum of water, as water tends to be a relatively strong absorber in the IR[8]. This absorption can be decreased by an order of magnitude by working in the O-band around 1310nm instead of the commonly used C-band around 1550nm. However, working at the shorter wavelength O-band will also cause increased modal confinement, and thus the role of water absorption vs. increased modal confinement at smaller wavelengths is in need of exploration.

Sensing performance of a microring resonator depends on both the waveguide material and dimensions, and will vary in performance depending on the light polarization and wavelength. For maximal sensing behavior, these parameters must be optimized with respect to one another and the desired analyte, and considering the effect they will have on the ring resonance shift and the ring's Q factor.

3. DEVELOPMENT OF A CROSS SECTIONAL MODEL

Because of the inherent three dimensional nature of the resonator, a full simulation of the device's performance requires a three dimensional model. However, since the shift in resonance is a result of the modal field interacting with the cell, this interaction can first be optimized, and then can be applied to the three dimensional model to save computing resources. A two dimensional cross section allows the effect of the waveguide material, waveguide dimensions, light polarization, and light wavelength to be explored. A model of the waveguide with a bound cell was developed in the commercial finite element modeling software COMSOL. A typical geometry of this cross section is shown in Fig. 1a.

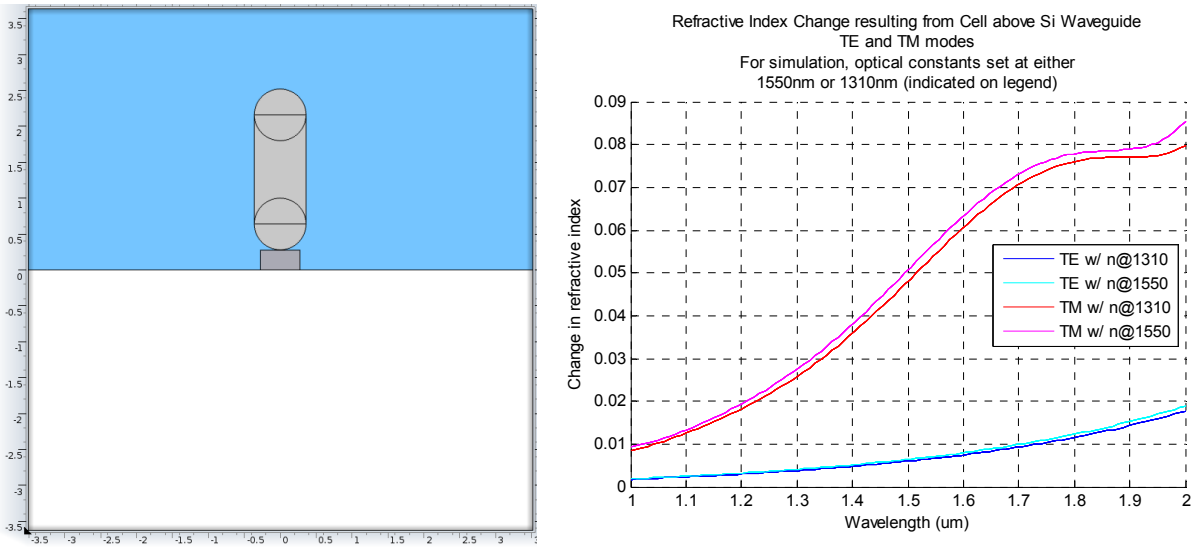

Figure 1: (a, left) Cross sectional model of ring and bound cell; (b, right) Refractive index change of 250x500nm (HxW) Si waveguide mode from cell

The model consists of a SiO_2 substrate, a Si or SiN waveguide, and a model cell surrounded by water. The design for the cell was based on parameters for the rod shaped *E. coli*.[9], with a total length of 2.24µm and a radius of 0.36µm. Refractive index for the cell was estimated to be 1.38 over the NIR[9]. The cell was placed 2nm directly above the ring with the cell axis perpendicular to the substrate. Additional binding geometries were also considered, and their performance was largely similar to that resulting from this perpendicular binding.

As an initial case, a silicon waveguide 500nm wide by 250nm high was simulated with input light 1-2µm in wavelength and polarized in either the TE or TM modes. The optical constants for materials were set at the values for either 1310nm or 1550nm[10], and the comparison between these cases is shown in Fig. 1b. It can be seen that, for both polarizations, shorter wavelengths see less of an index difference than longer wavelengths as a result of longer wavelength modes being less confined to the waveguide. Additionally, the reactive index difference is much higher for the TM modes than the TE modes. A comparison of the electric field intensity can be seen in Fig. 2. The large difference in refractive index change is a result of the TM field coupling significantly more of the field energy to the cell than the TE field.

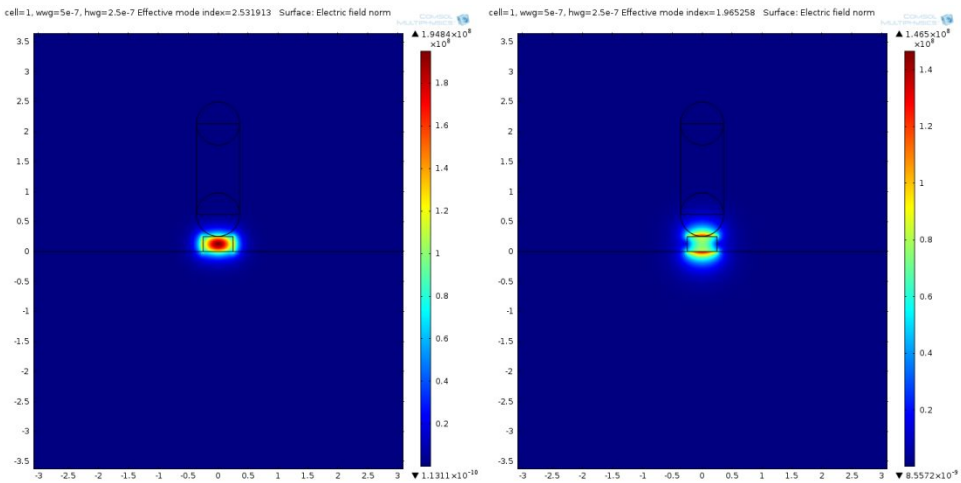

Figure 2: (a, left) TE polarized mode; (b, right) TM polarized mode, both in 250x500nm (HxW) Si waveguide

Although electric field profiles like these are often seen in literature on refractive index shift based sensing[3,7,8], they are inherently misleading. As was seen earlier, the refractive index shift does not depend only on the electric field, but the dot product of the electric field and the electric displacement field, which results in the energy density. A comparison of these field profiles is seen in Fig. 3.

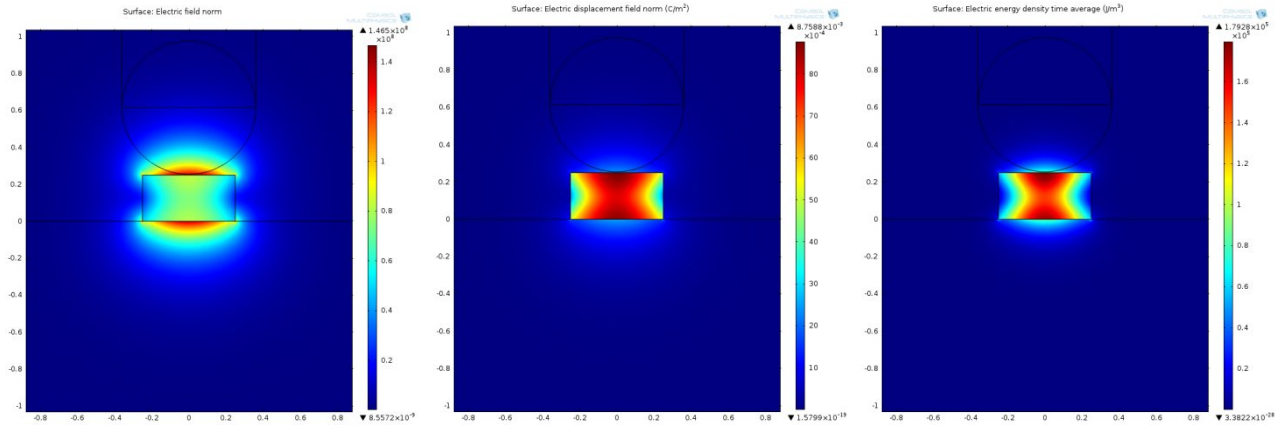

Figure 3: Electric field intensity (left), electric displacement field intensity (center), and the time averaged electric energy density for the same mode (right)

It is apparent that the actual sensing response of the waveguide is much less than would initially be assumed upon inspection of only the electric field. As energy density is essentially proportional to the square of the electric field ($\vec{D} \cdot \vec{E} = \varepsilon \left|\vec{E}\right|^2$), the sensing response is diminished accordingly. Thus, maximizing modal delocalization is extremely important to maximize the device sensitivity.

To maximize the effective index shift, the parameters of waveguide material, waveguide dimensions, light polarization, and light wavelength were varied. As the resulting index shift depends on the combination of these parameters, simulation was done over a full parameter range for each individual parameter. Both Si and SiN were tested at both the TE and TM polarization, each at 1310nm and 1550nm. For Si, the waveguide height was varied in 25nm steps from 100nm to 275nm, and the width in 50nm steps from 200nm to 550nm. For SiN, height was varied from 200nm to 600nm in 50nm steps, and width from 400nm to 1000nm in 100nm steps. A graph of the resulting index shift is shown below in Fig. 4. Note that the pure black squares indicate a waveguide geometry that does not support a propagating mode.

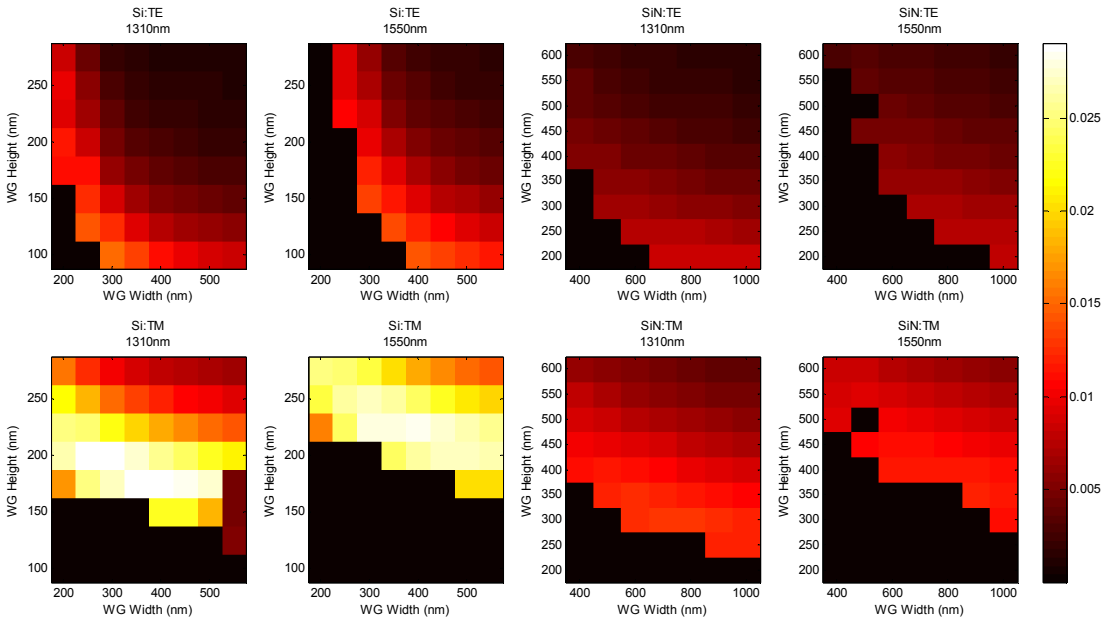

Figure 4: Refractive index shift due to cell for a variety of parameters

In all cases, TM provided higher sensitivity than TE, often by an order of magnitude. Si performed better than SiN, though only by a factor of 2-3 in most cases. The highest index shift was achievable in Si for the TM mode, operating at either 1310nm or 1550nm. For 1310nm, the maximum sensitivity came for heights between 175-200nm, and widths between 250-500nm. For 1550nm, best performance can be found for 200-250nm heights and 300-500nm widths.

4. THREE DIMENSIONAL RING OPTIMIZATION

Using the optimized parameters from the cross sectional case, a three dimensional model was developed. For the waveguide, Si was used, and excitation was done near 1550nm at the TM polarization. A height of 250nm and width of 500nm were used to maximize modal delocalization. An input/output waveguide was placed next to a 2.5μm radius ring resonator such that the ring was coupled in an all-pass fashion, which has been shown to offer better Q values than alternative ring coupling setups[2].

In order to allow the potential for proper simulation over a variety of wavelengths, the Sellmeier equation[10]:

$$n^2(\lambda) = 1 + \frac{B_1\lambda^2}{\lambda^2 - C_1} + \frac{B_2\lambda^2}{\lambda^2 - C_2} + \frac{B_3\lambda^2}{\lambda^2 - C_3}$$

was used in place of hard coded refractive index values (as was done in the cross sectional case) to define the refractive indices of Si, SiO_2, and H_2O[10]. For the cell, the value was left hard coded, as no Sellmeier coefficients could be found.

Performance was measured by simulating the ring at a variety of wavelengths, both with and without the cell, and finding the resonance peak of the ring for each case. In order to find the ring transmission spectrum, the integral of the power both before and after the ring was measured. The difference of these gave the transmission spectra.

As the waveguide and signal parameters had already been optimized, the main remaining parameter to optimize was the ring to waveguide coupling gap. It was found that the gap has little effect on the resonant wavelength, but a large effect on the coupled Q and extinction ratio of the ring (as is consistent with theory). A parameter scan can be seen in Fig. 5a, and it is apparent that a coupling gap between 150nm and 200nm offers the best extinction ratio. Using these values as bounds, the COMSOL optimization module was used to quickly find the coupling gap that offered the best performance. An optimal value of 168.5nm was found, and gave an extinction ratio of 7dB.

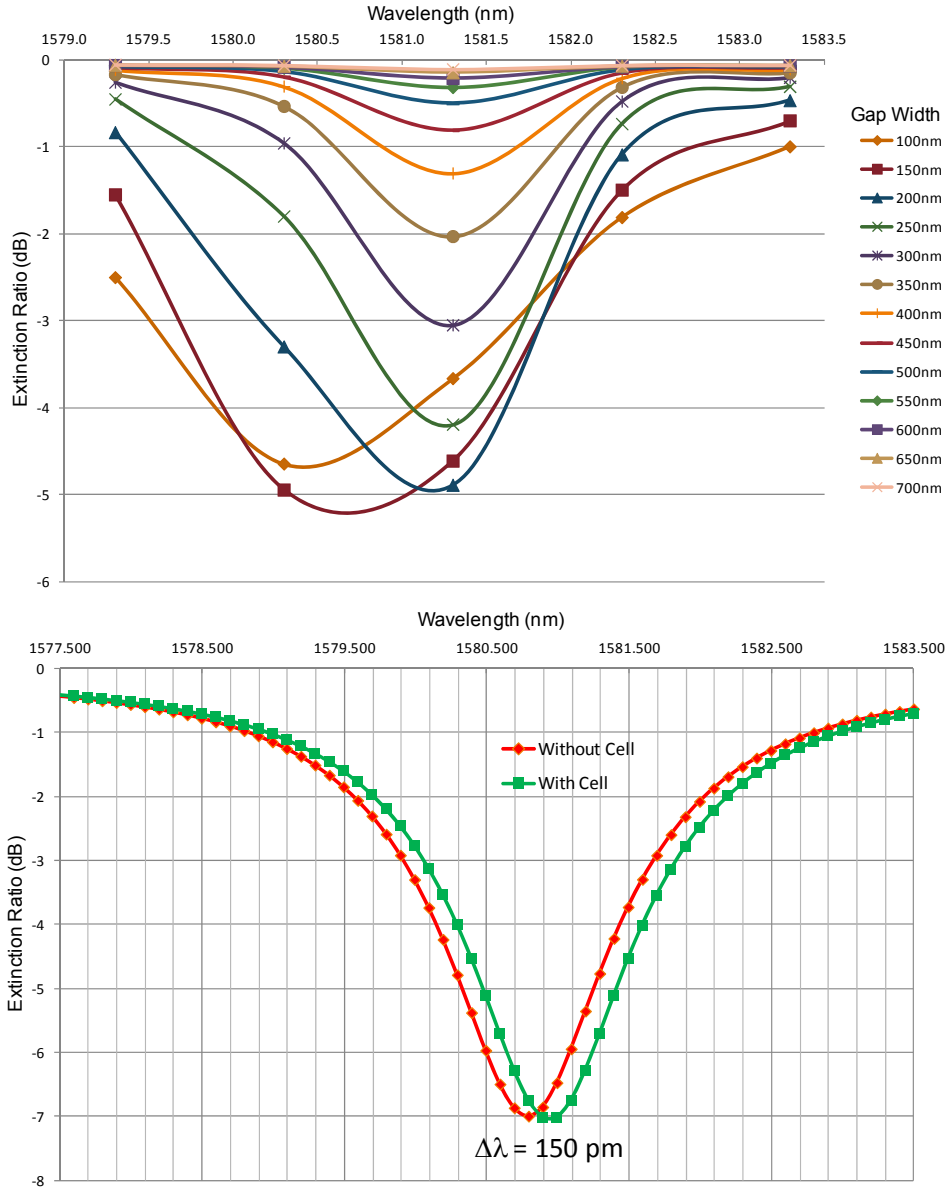

Figure 5: (a, top) Parameter sweep optimization of ring to waveguide coupling gap; (b, bottom) transmission spectra of ring resonator with and without a cell present

Simulating the ring coupling both with and without the ring with a coupling gap of 168nm, a wavelength shift of 150pm was found, and the resulting spectra are shown in Fig. 5b. The loaded Q of the ring was found to be 1215 with the cell, and 1245 without. At these levels, even a single cell would be easily detectable by the ring device, as much smaller wavelengths shifts have been measured experimentally[3,5,6].

5. DISCUSSIONS AND CONCLUSIONS

We have designed, numerically investigated, and optimized a microring resonator for use as a biological sensor. Starting with a two dimensional cross sectional model of a cell binding to a waveguide, the waveguide material, waveguide dimensions, light wavelength, and light polarization were investigated. It was found that silicon waveguides operating in the TM polarization offer maximum performance, and that depending on the wavelength of light used, the dimensions can be adjusted for optimum sensitivity. A waveguide optimized cross section was then used in a three dimensional model of a single cell binding with a ring resonator. It was found that, for a 2.5μm radius ring resonator, a 150pm shift

was achievable with a quality factor over 1200. Thus, it was concluded that detection of a cell with the optimized resonator design provided performance more than adequate for single cell detection.

6. ACKNOWLEDGEMENTS

The authors are thankful for the funding support through the Air Force Research Laboratory (AFRL) Sensors Directorate 2012 Entrepreneurial Research Funds.

REFERENCES

[1] Heyn, P. De, and Kuyken, B., "High-performance low-loss silicon-on-insulator microring resonators using TM-polarized light," in Optical Fiber Communication Conference, OSA Technical Digest (CD) (Optical Society of America, 2011), paper OThV2.
[2] Bogaerts, W., De Heyn, P., Van Vaerenbergh, T., De Vos, K., Kumar Selvaraja, S., Claes, T., Dumon, P., Bienstman, P., Van Thourhout, D., et al., "Silicon microring resonators," Laser & Photonics Reviews 6(1), 47–73 (2012).
[3] Xu, D.-X., Vachon, M., Densmore, A., Ma, R., Janz, S., Delâge, A., Lapointe, J., Cheben, P., Schmid, J.H., et al., "Real-time cancellation of temperature induced resonance shifts in SOI wire waveguide ring resonator label-free biosensor arrays," Optics Express 18(22), 22867–79 (2010).
[4] De Vos, K., Bartolozzi, I., Schacht, E., Bienstman, P., and Baets, R., "Silicon-on-Insulator microring resonator for sensitive and label-free biosensing," Optics Express 15(12), 7610–5 (2007).
[5] De Vos, K., Girones, J., Popelka, S., Schacht, E., Baets, R., and Bienstman, P., "SOI optical microring resonator with poly(ethylene glycol) polymer brush for label-free biosensor applications," Biosensors & Bioelectronics 24(8), 2528–33 (2009).
[6] Iqbal, M., Gleeson, M., and Spaugh, B., "Label-free biosensor arrays based on silicon ring resonators and high-speed optical scanning instrumentation," IEEE JSTQE 16(3), 654–661 (2010).
[7] Densmore, A., Xu, D., and Waldron, P., "A silicon-on-insulator photonic wire based evanescent field sensor," IEEE PTL 18(23), 2520–2522 (2006).
[8] Vos, K. de, "Label-free Silicon Photonics Biosensor Platform with Microring Resonators," Ph.D. dissertation, Univ. Gent, Gent, Belgium (2010).
[9] Balaev, A.E., Dvoretski, K.N., and Doubrovski, V.A., "Determination of refractive index of rod-shaped bacteria from spectral extinction measurements," Proc. SPIE 5068, 375–380 (2003).
[10] Tan, W.C., Koughia, K., Singh, J., and Kasap, S.O., [Optical Properties of Condensed Matter and Applications] , J. Singh, Ed., John Wiley & Sons Ltd, 1-23 (2006).